Ref. Ares(2024)3784845 - 27/05/2024

AI-informed Holistic Electric Vehicles Integration Approaches for Distribution Grids

D3.2

E-mobility Flexibility Models

January 2026 (M20)

Co-funded by the European Union

This project has received funding from the European Union's Horizon Europe research and innovation programme under grant agreement No. 101160665.

DELIVERABLE DETAILS					
Project	AHEAD	Grant Agreement	101160665		
Deliverable Type (R, DEM, DEC)	R	Deliverable Title	E-Mobility Flexibility Models		
Status	Draft	Month due	M20	Date	31/01/2026
Lead author(s)	Blaž Dobravec (EG), Lenart Ribnikar (EG)				
Co-author(s)	Karel Križnar (EG), Julian Marius Mittag (DTU)				
Peer reviewer(s)	Rui Martins (EEM)				
Dissemination level	PU - Public				

HISTORY OF CHANGES				
Document history	Date	Version	Submitted by	Comments
	01/08/2025	V0.1	EG	Initial content
	10/10/2025	V0.2	EG	The initial version of the methodology and input parameters.
	01/11/2025	V03	EG	Main body content, simulations of the methodology and the examples.

	28/11/2025	V0.4	EG	Added the corrections and updated proposed by the Task partners. Performed the cleanup.
	14/01/2026	V0.5	EG	Resolved any comments by internal review team and spelling correction.
	26/01/2026	V1.0	POLIMI	Uploaded document

LEGAL DISCLAIMER:

This project has received funding from the European Union's Horizon Europe research and innovation programme under grant agreement No. 101160665.

Views and opinions expressed are however those of the author(s) only and do not necessarily reflect those of the European Union or CINEA. Neither the European Union nor the granting authority can be held responsible for them.

EXECUTIVE SUMMARY

Deliverable D3.2 defines a practical modelling framework to represent e-mobility flexibility in a form directly usable for distribution grid planning, congestion management, and flexibility activation within AHEAD. It focuses on turning stochastic EV charging behaviour into probabilistic net-load profiles and flexibility envelopes that can be exchanged with other work packages.

The framework combines: (i) stochastic models for arrivals, dwell times, energy requests, initial SoC and temperature effects by segment (home, work, public, fleet); (ii) charger-level flexibility envelopes under three control modes—uncontrolled, smart unidirectional (V1G), and optional bidirectional (V2G); and (iii) aggregation methods that include diversity factors, correlation structures, and realistic synchronisation and rebound effects. Deterministic envelopes are converted into probabilistic (and optionally quantile-based) envelopes, providing compact, machine-readable inputs for probabilistic load-flow and hosting-capacity analyses.

An illustrative example shows how different control strategies reshape peaks and available flexibility, demonstrating how the approach links operational behaviour with planning-grade representations. The models and data structures specified here provide the methodological basis for the tools to be developed in Task 3.4 and supply WP4 and WP6 with consistent flexibility artefacts for evaluating EV integration strategies in European distribution grids.

TABLE OF CONTENTS

LIST OF FIGURES

LIST OF ACRONYMS

AHEAD	AI-informed Holistic Electric Vehicles Integration Approaches for Distribution Grids
DSO	Distribution System Operator
EV	Electric Vehicle
EVSE	Electric Vehicle Supply Equipment (charger)
V1G	Smart Unidirectional Charging
V2G	Vehicle-to-Grid (Bidirectional Charging)
SoC	State of Charge
TOU	Time-of-Use Tariff
PLF	Probabilistic Load Flow
GDPR	General Data Protection Regulation
AMI/SM	Advanced Metering Infrastructure / Smart Meter
WP	Work Package
O1–O6	Objectives defined in Deliverable D3.2
Δt	Simulation time step

1. INTRODUCTION

The rapid electrification of road transport is reshaping demand on European distribution grids. Electric Vehicles (EVs) introduce new, flexible but stochastic loads whose timing, location, and controllability depend on human behaviour, weather, prices, and charging infrastructure. Distribution System Operators (DSOs), aggregators, and energy communities need models that translate these behaviours into planning-grade inputs and activation-grade flexibility descriptions. **Deliverable D3.2, E-Mobility Flexibility Models**, specifies a modelling framework that enables probabilistic grid planning while remaining robust and flexible enough to be adopted by planners.

1.1. Scope and Objectives

Deliverable D3.2 defines and delivers simulation models of e-mobility flexibility for use in grid planning methodologies, reflecting dynamic behaviours of e-mobility and the requirements of probabilistic grid planning methods. The scope spans: (i) demand modelling for arrivals, dwell times, and energy needs across home/work/public contexts; (ii) representation of flexibility (V1G baseline and smart-charging control, with optional V2G placeholders) as time-coupled envelopes; (iii) price and control response functions capturing user heterogeneity and adoption rates; and aggregation and scenario reduction to produce tractable inputs for the planning tools.

Deliverable D3.2 pursues the following concrete objectives:

- **O1 — Demand model.** Specify stochastic processes for arrivals, dwell durations, initial state-of-charge (SoC), and energy requests, differentiated by location type and charger class, with seasonal and weather dependencies.
- **O2 — Flexibility envelopes.** Define time-based charging trajectories (min/max power profiles) that respect SoC dynamics, charging limits, and availability windows; provide reduced-order, planner-friendly approximations.
- **O3 — Synchronisation and rebound.** Model avalanche effects and deferred-energy rebound through backlog state variables, ramp constraints, and queue-clearing dynamics to prevent underestimation of post-event impacts.
- **O4 — Aggregation & correlation.** Specify methods to convolve individual EVSE/EV behaviours to EVSE charging park level, including diversity factors and correlation structures across sites and time.

- **O5 — Calibration & validation.** Identify parameters to be calibrated from charging logs, mobility surveys, and smart-meter (AMI/SM) data; define validation criteria vs. observed loads and session statistics.
- **O6 — Reproducibility & GDPR compliance.** Provide open, reproducible examples and anonymisation/aggregation guidance consistent with GDPR and data-sharing agreements.

1.2. Structure

The remainder of the deliverable is organised as follows:

- **Section 2 — Background & Related Work.** Summarises current state-of-the-art research on the EV charging and flexibility modelling, price responsiveness, synchronisation and rebound risks, seasonal/weather coupling and planning needs.
- **Section 3 — Modelling Framework Overview.** Presents the layered architecture from models through envelopes and clustering to the grid coupling and flexibility service integration.
- **Section 4 — Flexibility Representation.** Formalises stochastic arrivals/dwell, energy demand/SoC, price/control response, control modes (uncontrolled, V1G, optional V2G); provides core equations and parameters for calibration as well as provides an example for the individual scenario.
- **Section 5 — Conclusions.** Summarises key findings and practical overview of the deliverable.

1.3. Relationship with other deliverables

Deliverable D3.2 bridges flexibility modelling in WP3 with planning-centric analytics in WP6 and supports flexibility activations in WP4. Its role in the AHEAD ecosystem is to convert heterogeneous data into planner-ready inputs and flexibility artefacts. In particular:

- Consumes inputs from:
    - Use-case and requirements definitions (e.g., target network constraints, user segments, charging contexts).
    - Data acquisition & harmonisation activities carried out in Task 1.1 (charging session logs across home/work/public, AMI/SM data, weather and calendar data, tariffs/prices).
    - Market analysis relevant to tariffs, incentives, and control signals.
    - Ethics/GDPR guidance for anonymisation, aggregation, and k-anonymity thresholds.
- Provides outputs to:
    - WP6 Probabilistic Planning: Probabilistic net-load profiles per node, flexibility envelopes, price-response functions suitable for hosting-capacity and risk analyses.
    - WP4 Demonstrations & Field Trials: Baseline vs. smart-charging trajectories/predictions, parameter ranges for controllers, and test scenarios capturing synchronisation and rebound dynamics.
    - WP5 Markets & Operation: Inputs to evaluate the value of flexibility under different tariff/market designs and DSO signal schemes.

2. BACKGROUND & RELATED WORK

2.1. Charging behaviour & priceresponsiveness

Evidence consistently shows a **home-dominant baseline**, with **workplace** charging creating a strong **midday** opportunity (solar alignment) and **public** charging being a smaller but critical complement for long trips and apartment dwellers. Large UK smart-charging trials (Electric Nation, ~700 participants) and syntheses of charging datasets found that unmanaged home charging clusters in the evening, while managed/home time-of-use (TOU) nudges shift load overnight [1]; workplace programs can move energy to midday but responses are weaker than at home [2].

A recent field study of workplace charging at UC San Diego reports that a 50% price discount increased energy by ~22%, implying a workplace price elasticity ≈ −0.44; by contrast, home off-peak timing elasticity is much larger (~ −1.6) in comparable experiments, i.e., people respond more strongly to prices that shift when they charge at home than to incentives to where they charge [3].

Multiple trials and field experiments show TOU/dynamic incentives can cut peak-hour charging dramatically, e.g. **~49% reduction in peak-period charging** in a randomized experiment; however, simple "start at cheap hour" rules can **synchronize** starts at the TOU boundary (e.g., 00:00–01:00), creating **secondary peaks** unless diversified or actively controlled [4].

Emerging pilots indicate that **dynamic pricing plus automated smart charging** keeps a very high share of energy off-peak (reports up to **~98% off-peak**), outperforming static TOU alone—supporting AHEAD's emphasis on controller-friendly response functions rather than price-only heuristics [5].

Uncoordinated home charging measurably **reshapes residential load** and can stress local assets even at modest EV shares; stepwise TOU (without diversity/randomization) can **increase** peak loads versus purely on-arrival charging. This motivates flexibility models that (i) include **correlated start times**, and (ii) allow **randomization/queueing** to desynchronize responses [6] [7].

2.2. Synchronization risks

Synchronization occurs when many EVs react in the same way to a common signal or rule—for example, all starting to charge as soon as an off-peak tariff begins or when an algorithm identifies the same cheapest interval. The result can be a new coincident peak (an "avalanche"), followed by a concentrated recovery in demand after a curtailment event (a "rebound"). Distribution-level studies and trials show that simple TOU pricing and uniform control rules can create secondary or even 'super-' peaks unless diversity is engineered into the response [8].

Three mechanisms drive these effects. First, market signals with sharp boundaries—midnight TOU roll-overs or step changes in real-time prices—invite timer-based behaviour and simultaneous starts; several utility and research studies document 'shadow peaks' immediately after the off-peak begins. Second, identical cost-minimising algorithms concentrate actions in the same interval when they optimise on the same data without local network constraints, a behaviour reproduced in urban network simulations [9]. Third, user routines (evening arrivals and long overnight dwell times) naturally align availability windows; a uniform off-peak rule amplifies this coincidence [9].

Field and modelling evidence is consistent. An NREL analysis of EV customer response to TOU rates across ten distribution systems shows that TOU can shift load off the system peak but also create secondary peaks at the rate boundary under higher adoption, unless active control or randomisation is applied [8].

Rebound arises when energy delivery is deferred by curtailment or congestion management: the unmet charging obligation accumulates as a backlog and is then repaid when constraints relax. Demand-response literature reports snapback behaviour after events; EV-specific demonstrations show charging power can overshoot immediately after a temporary disconnection before settling, if no ramping or queueing is enforced [10] [11]. This dynamic is crucial for planning because it can shift stress from the peak hour to the recovery window and stack with other flexible loads.

A credible distribution-planning risk when controllers ignore local constraints or when many users follow identical rules; incorporating heterogeneity and grid-aware objectives reduces overload risk [8].

2.3. Seasonal & weather correlation

EV charging demand is seasonal and weather-sensitive along three channels: (i) underlying mobility demand that shapes arrival and dwell distributions; (ii) temperature-dependent vehicle efficiency and charging behaviour; and (iii) co-variation with other electric loads and distributed generation. In this report we will mainly focus on the first two. Together these factors determine both baseline and flexible charging through the year, which must be reflected in planning-grade models [12] [13].

Mobility exhibits clear seasonality. Empirical travel-behaviour research for Europe finds that winter conditions reduce outdoor activity windows and shift time allocation towards home in the evenings, whereas longer daylight in summer supports more daytime activity away from home—implying longer evening/home dwells in winter and more midday destination/work dwells in summer. These patterns have been quantified in longitudinal and seasonal travel-demand studies and are consistent with national travel statistics [12] [14]. For modelling, this means arrival and departure distributions, and the mix of home versus workplace/public charging, should be segmented by season.

Ambient temperature affects EV energy per kilometre and the timing/length of sessions. Laboratory and field studies show that cold conditions increase energy use for battery and cabin heating, while extreme heat increases air-conditioning loads. AAA's controlled tests reported an average ~41% range reduction at 20°F (−6.7°C) when cabin heat is used, with much smaller impacts at 95°F (35°C) (~4–5%). A 2024 U.S. Department of Energy synthesis and 2025 NREL assessment corroborate higher energy use and reduced range in cold weather, and show that heat-pump-equipped vehicles lose less range than vehicles with resistive heaters at sub-zero temperatures [15]. In practice, colder days therefore raise daily energy needs and can lengthen or shift charging sessions due to pre-conditioning and reduced effective charging rates [16]. Planning tools should therefore treat temperature as a driver EV energy demand.

2.4. EV location planning requirements

Spatially explicit identification of EV charging infrastructure sites requires the integration of mobility demand modelling with grid and land-use constraints covered in the previous paragraph. Probabilistic extensions incorporate uncertainty in vehicle arrivals, dwell times, and adoption rates, combining traffic assignment or agent-based mobility simulations with stochastic load-flow analysis to quantify local hosting limits.

Planning of the EV charging infrastructure under high EV penetration requires models that quantify risk—not just point estimates on the side of grid planners and also requires the identification of geographically sound and viable options. In practice, grid planners need probabilities of violating feeder thermal, voltage and transformer constraints under uncertain arrivals, dwell times, energy needs and non-EV coincident loads. Two families of approaches are commonly used: (i) scenario-based Monte Carlo pipelines that propagate uncertainty through load flow, and (ii) analytical/approximate probabilistic load-flow (PLF) methods that compute output distributions more efficiently than brute-force sampling [17] [18]. This deliverable focuses on the first one.

Scenario-based methods are transparent and flexible, but computationally heavy. To keep runtimes tractable, stochastic-programming practice relies on **scenario reduction** and **heuristics definition** that approximate the full distribution over the horizon. Classical algorithms by Dupačová and by Heitsch & Römisch [19] minimise transportation-metric distances between the original and reduced measures and provide guarantees and practical heuristics for multistage trees [20]. For annual studies, time-series aggregation to **representative periods** (days/weeks) via clustering or optimisation is also widely used; best-practice guides emphasise optimisation outcomes on the full series and ensuring extremes/ramping are captured via weighting or linkage between periods [21] [22] [23]. We use k-medoids clustering on daily net-load/EV-connectivity profiles with Wasserstein distance.

Geographic Information System (GIS) layers are frequently employed to filter candidate sites based on accessibility, zoning, and network connectivity, while clustering of expected charging demand guides site prioritisation [24] [25]. Hybrid frameworks combining spatial clustering, probabilistic network analysis, and chance-constrained optimisation have been shown to balance computational tractability with risk-aware siting performance, supporting planners in identifying geographically viable and grid-compatible charging locations [26].

3. MODELLING FRAMEWORK OVERVIEW

The modelling framework developed under Deliverable D3.2 provides a unified structure for translating heterogeneous behavioural data into probabilistic flexibility artefacts suitable for grid-planning and hosting-capacity analyses. It integrates stochastic models, reduced-order flexibility envelopes and scenario generation. The design aligns with the AHEAD objective of enabling probabilistic yet computationally tractable representations of e-mobility flexibility across spatial and temporal scales.

At its core, the framework consists of five layers:

1. **Demand modelling.**

   Individual EV charging sessions are modelled as stochastic processes describing arrivals, dwell durations, and energy requests, conditional on location type (home, work, public) and contextual factors (season, weekday, temperature, price[1]). Inhomogeneous Poisson or renewal processes capture the time-varying arrival intensity, while conditional distributions of dwell and requested energy incorporate user heterogeneity and weather dependence. Parameters of the individual distributions are calibrated using charging session data in multiple locations across Europe (in the Task 3.3), ensuring representativeness across demographic groups and geographic regions.

2. **Flexibility representation.**

   For each charging session, feasible power trajectories P_t are bounded by *time-coupled envelopes* $\left[P_t^{\min}, P_t^{\max}\right]$ consistent with SoC dynamics and charger ratings. When available the boundaries are set by the difference between the charging and parking time on the charger level as well as the charger max power. The envelopes encapsulate flexibility ranges under uncontrolled (baseline), smart-charging (V1G), and optional bidirectional (V2G) modes.

3. **Aggregation and correlation.**

   Individual EV/EVSE models are convolved at charging parks and feeder/substation level (grid perspective) using diversity factors and empirically derived correlation structures. This step produces **aggregate flexibility envelopes** that reflect realistic coincidence levels among users while preserving extreme-event behaviour. Temporal

[1] With price, we refer to the cost of charging in this deliverable. This cost can be composed of the spot price, grid tariffs, electricity retailer fees, charge point operator surcharges and taxes. Dynamic pricing in any of these components can be an incentive for the EV user to minimize charging costs.

correlations (e.g., daily and weekly routines) are maintained through cluster-based sampling of representative periods.

4. **Flexibility service activation signals.**

While heuristics can efficiently propagate uncertainties in arrivals, dwell times, and user responses through aggregated models to generate probabilistic net-load trajectories, fully stochastic optimisation remains computationally intensive. Therefore, the proposed methodology adopts a heuristic formulation in which the objective function and decision logic are defined for each specific flexibility service use case. This structure balances computational tractability with sufficient accuracy for planning and activation analyses.

The layered design ensures modularity: consumption models can evolve independently of grid tools, while the envelopes provide the grid planners with consistent consumption boundary. The framework enables DSOs and planners to explore the probabilistic impacts of e-mobility under uncertainty in a transparent and reproducible manner.

4. FLEXIBILITY REPRESENTATION

Flexibility models describe what each EV (or EVSE) can do, is likely to do without control, and will do under a given control or price signal, at operational time scales (minutes to hours). The representation must:

- preserve key stochastic features of arrivals, dwell times, and energy needs;
- remain computationally light enough for integration into large-scale scheduling and congestion-management tools;
- expose control-relevant parameters (e.g. maximum deferrable energy, ramp rates, rebound risk) in a transparent way.

In AHEAD, flexibility is built in three steps:

5. Stochastic availability driven by historical arrivals and dwell times (Section 4.1).
6. Service request and initial state of charge (Section 4.2).
7. Pricing and grid request (Section 4.3).
8. Operational control modes that define feasible sets of trajectories (Section 4.4) which are simplified to accommodate the planning activities.

The output is a set of time-coupled feasible trajectories and associated probabilities for each controllable entity (EV, EVSE, or aggregated cluster). These artefacts can be:

- directly optimised by centralised schedulers (e.g. DSO/aggregator control),
- or embedded into local controllers as policies consistent with system-level objectives.

4.1. Stochastic arrivals & dwell

This subsection defines how availability is modelled: when an EV is plugged in and can respond to activation signals. We distinguish location/usage types:

- home & multi-unit residential,
- workplace & depot,
- public slow/normal AC,
- public fast/ultrafast,
- special fleets (logistics, buses, taxis) where applicable.

For each segment, we represent arrivals and dwell times using inhomogeneous stochastic processes calibrated on empirical data. The goal is to generate, for each EV/EVSE i:

- a random connection interval $\left[T_i^{\text{arr}}, T_i^{\text{dep}}\right]$,
- an associated **availability indicator** $a_{i,t} \in 0{,}1$, where $a_{i,t} = 1$ if the EV is plugged and eligible for control.

4.1.1. Arrival process

For a given segment s (e.g. “home, weekday, winter”) and charger j, arrivals are modelled as an *inhomogeneous Poisson* or renewal process:

$$N_{s,j}(t) \sim \text{Poisson}\left(\int_0^t \lambda_{s,j}(u)\ du\right),$$

where $\lambda_{s,j}(t)$ is the time-varying arrival rate, conditioned on (depending on the data availability):

- day type (weekday/weekend/holiday),
- season (summer, winter, autumn, spring),
- weather (e.g. temperature bins),
- socio-demographic and mobility characteristics of the catchment area, including land use and proximity to key facilities,
- charger type.

This structure captures realistic clustering of arrivals (e.g. evening home arrivals). Within the Task 3.3 we identified the optimal clusters and the corresponding distributions based on the available data. The centroids of the clusters can directly be used when no charging session pattern data is available.

4.1.2. Dwell time distribution

Conditional on an arrival at time $\mathrm{T_i^{arr}} = \mathrm{t}$, the dwell time:

$$\Delta T_i = T_i^{\text{dep}} - T_i^{\text{arr}}$$

is modelled using a parametric or semi-parametric distribution:

$$\Delta \mathrm{T_i} \sim \mathrm{f_s}(\ \cdot \mid \mathrm{T_i^{arr}}, \text{context}),$$

where “context” may include:

- location type (home/work/public/depot),
- charger type (AC slow, DC fast, etc.),
- day type and season,
- temperature and weather,

- known schedule information (e.g. working hours, fleet timetables).

Typical choices for f_s are lognormal, Weibull or mixture distributions, selected based on goodness-of-fit to empirical session data. For fleets or structured users, deterministic or narrow-band distributions (e.g. fixed working shifts) can be used.

4.1.3. Availability indicator

For each simulated or observed session i:

$$\mathrm{a_{i,t}} = 1 \text{ if } \mathrm{T_i^{arr}} \leq \mathrm{t} < \mathrm{T_i^{dep}}, \text{ else } 0$$

At the level of an EVSE or node j, the number of connected vehicles at time t is:

$$\mathrm{A_j(t)} = \sum_{\mathrm{i} \in \mathcal{I}_j} \mathrm{a_{i,t}}.$$

This quantity underpins the feasible charging capacity at j and the maximum upward/downward flexibility for activation services at each time step. Within AHEAD, the arrival and dwell models are calibrated:

- per segment (home/work/public/fleet),
- per geographical region,
- per day type and season;

The resulting availability processes feed directly into the following sections, where flexibility envelopes are constructed *conditional on* $\mathrm{a_{i,t}}$.

4.2. Energy request & initial SoC

The **energy request** E_i^{req} represents the amount of energy an EV aims to charge during a session.

It depends on the preceding trip length L_i, the dwell duration $\Delta T_i = T_i^{dep} - T_i^{arr}$, and contextual factors such as temperature and season. For each segment s (home, work, public, fleet):

$$E_i^{req} \sim g_s(\cdot \mid L_i, \Delta T_i, \text{vehicle type}, \text{season}, \theta_i)$$

A simple physical relation is (energy missing on arrival):

$$E_i^{req} = \frac{L_i}{\eta_i^{drv}(\theta_i)} + E_i^{aux}(\theta_i)$$

where $\eta_i^{drv}(\theta_i)$ denotes temperature-dependent driving efficiency and $E_i^{aux}(\theta_i)$ accounts for auxiliary heating/cooling and preconditioning. Feasibility is enforced by:

$$0 \leq E_i^{req} \leq P_i^{max} \, \Delta T_i$$

The **initial state of charge** on arrival is:

$$\mathrm{SoC}_{i,0} = 1 - \frac{E_i^{req}}{E_i^{bat}} + \varepsilon_i, \varepsilon_i \sim \mathcal{N}\left(0, \sigma_{\mathrm{SoC}}^2\right)$$

with a min/max constraint:

$$\mathrm{SoC}_{i,0} = \min\left(1,\ \max\left(0,\ 1 - \frac{\mathrm{E_i^{req}}}{\mathrm{E_i^{bat}}} + \varepsilon_\mathrm{i}\right)\right)$$

Lower temperatures increase energy use and reduce $\mathrm{SoC}_{i,0}$, while workplace or daytime arrivals in summer generally yield higher initial SoC values. Typical mean values are ≈ 0.35–0.45 (home), 0.45 (workplace), and 0.25 (public).

During operation, SoC evolves as:

$$\mathrm{SoC}_{i,t+1} = \mathrm{SoC}_{i,t} + \frac{\eta_i^{drv} P_{i,t} \Delta t}{E_i^{bat}}, 0 \leq P_{i,t} \leq P_i^{max} a_{i,t}, \mathrm{SoC}_{i,T_i^{dep}} \geq \mathrm{SoC}_i^{target}$$

4.3. Price & control response

The **price and control response** describes how EV charging power reacts to electricity prices or external control signals. It determines how much of the available charging capacity is used at time t. A simple behavioural model is defined as:

$$P_{i,t}^{req} = P_i^{max} \cdot \sigma(\alpha_i + \beta_i \pi_t + \gamma_i c_t)$$

where

- $P_{i,t}^{req}$ — requested charging power [kW],
- P_i^{max} — rated charger power,
- π_t — price or tariff signal,
- c_t — control signal (e.g. DSO or aggregator command),
- α_i — baseline charging tendency,
- β_i — price sensitivity,
- γ_i — control responsiveness,
- $\sigma(x) = 1/(1 + e^{-x})$ — logistic response function.

The parameters β_i and γ_i capture user behaviour:

- **Uncontrolled:** $\beta_i, \gamma_i \approx 0 \rightarrow$ always charges on arrival.
- **Smart (V1G):** negative $\beta_i \rightarrow$ shifts load to low-price hours.
- **Controlled (aggregated):** positive $\gamma_i \rightarrow$ follows system signals.

Finally, instantaneous charging power is bounded by availability:

$$0 \leq P_{i,t} \leq P_i^{max} \, a_{i,t}$$

4.4. Control modes

Control modes define how the charging power $P_{i,t}$ is realised from the underlying availability, energy request, and response functions. They represent distinct operational behaviours that together determine the **feasible set of charger-level power trajectories** used for activation and planning. For each vehicle or charger i, the instantaneous charging power is:

$$P_{i,t} = a_{i,t} \cdot f_i\left(E_i^{req}, \mathrm{SoC}_{i,t}, \pi_t, c_t\right)$$

where

- $a_{i,t}$ = availability indicator (from Section4.1),
- E_i^{req} = energy request (from Section 4.2),
- $\mathrm{SoC}_{i,t}$ = current state of charge,
- π_t, c_t = price and control signals (from Section 4.3).

The function $f_i(\cdot)$ defines how the charger operates under different control modes.

4.4.1. Uncontrolled charging (baseline)

The uncontrolled mode represents standard plug-and-charge behaviour, without price or control feedback:

$$P_{i,t}^{base} = \begin{cases} P_i^{max}, & a_{i,t} = 1 \text{ and } \mathrm{SoC}_{i,t} < \mathrm{SoC}_i^{target}, \\ 0, & \text{otherwise.} \end{cases}$$

Energy is delivered continuously at rated power until the target SoC is reached or the vehicle departs. This mode is used as the reference case for flexibility quantification.

4.4.2. Smart charging (V1G)

In smart charging (V1G) mode, charging is optimised or adjusted in response to tariffs or control signals, but remains unidirectional. The feasible set of charging profiles is:

$$\mathcal{F}_i = \{P_{i,t} \mid 0 \leq P_{i,t} \leq P_i^{max} a_{i,t},\ \mathrm{SoC}_{i,t+1} = \mathrm{SoC}_{i,t} + \frac{\eta_i^{ch} P_{i,t} \Delta t}{E_i^{bat}},\ \mathrm{SoC}_{i,T_i^{dep}} \geq \mathrm{SoC}_i^{target}\}$$

Smart charging typically minimises cost or follows a DSO signal:

$$\min_{P_{i,t} \in \mathcal{F}_i} \sum_t (\pi_t + c_t) P_{i,t}$$

V1G thus shifts charging to off-peak periods or to times beneficial for the grid while ensuring the required energy is delivered before departure.

4.4.3. Bidirectional charging (V2G)

The *V2G* mode extends V1G by allowing power export within rated inverter limits:

$$-P_i^{dis,max} a_{i,t} \le P_{i,t} \le P_i^{ch,max} a_{i,t}$$

The SoC update then includes both charging and discharging efficiencies:

$$\mathrm{SoC}_{i,t+1} = \mathrm{SoC}_{i,t} + \frac{\eta_i^{ch} P_{i,t}^{+} \Delta t}{E_i^{bat}} - \frac{P_{i,t}^{-} \Delta t}{\eta_i^{dis} E_i^{bat}}$$

where $P_{i,t}^{+} = \max(P_{i,t}, 0)$ and $P_{i,t}^{-} = \max(-P_{i,t}, 0)$. V2G participation is typically optional and limited to fleet or controlled environments due to battery-wear and user constraints (subset of the simulated V2G vehicles and chargers is represented in Figure 1).

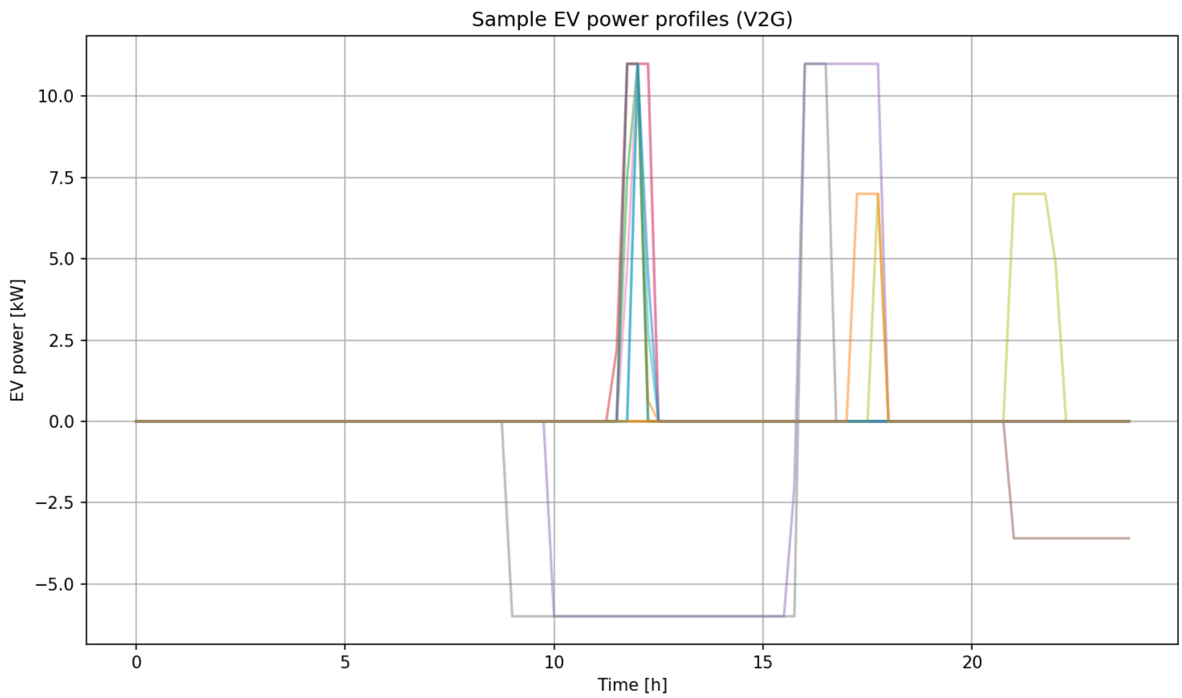

Figure 1: Representative charger-level trajectories for a subset of V2G-capable EVs, showing bidirectional behaviour: discharging during high-price or constrained hours and recharging at favourable times, subject to state-of-charge limits.

4.4.4. Charger-level output definition

The realised charger-level power is determined by the control mode:

$$P_{i,t} = \begin{cases} P_{i,t}^{base}, \text{uncontrolled}, \\ P_{i,t}^{opt}, \text{smart charging (V1G)}, \\ P_{i,t}^{bi}, \text{bidirectional (V2G)}. \end{cases}$$

For aggregation, the EV Charging park power is:

$$P_{j,t}^{agg} = \sum_{i \in \mathcal{I}_j} P_{i,t}$$

These aggregated trajectories serve as the flexibility inputs for WP4 activations and WP6 probabilistic planning.

4.5. Flexibility Representation for Planning

The activation-level model developed in Sections 4.1 – 4.4 defines, for each electric vehicle or charger i, a feasible set of power trajectories $P_{i,t}$ that satisfy stochastic availability, energy, and state-of-charge (SoC) constraints. While these activation models describe short-term behaviour under operational signals (minutes to hours), **planning applications** require reduced, computationally tractable representations that summarise the same flexibility characteristics across longer horizons (days to years). This subsection describes how activation-level results are transformed into **planning-level flexibility representations** suitable for network studies, hosting-capacity analyses, and probabilistic reinforcement deferral assessments.

Each simulated trajectory $P_{i,t}$ under a given control mode (uncontrolled, V1G, V2G, peak-reduction) defines a feasible region of operation bounded by:

$$P_{i,t}^{\min} \leq P_{i,t} \leq P_{i,t}^{\max},$$

where the limits correspond to the extreme charging and discharging powers compatible with the SoC evolution and the availability window $a_{i,t}$.

Aggregating across all controllable assets at node j yields the **Charging-park-level flexibility envelope** (flexibility envelope shows the feasible kW range over time; the probabilistic version accounts for average EV connection rates.):

$$P_{j,t}^{\min} = \sum_{i \in \mathcal{I}_j} P_{i,t}^{\min}, P_{j,t}^{\max} = \sum_{i \in \mathcal{I}_j} P_{i,t}^{\max}.$$

The pair $[P_{j,t}^{\min}, P_{j,t}^{\max}]$ represents the **instantaneous upward and downward flexibility margins** of the node or substation, conditioned on user availability and system state. These envelopes can be interpreted as the feasible range of grid import/export power at each time step.

4.5.1. Probabilistic Availability and SoC Coupling

The stochastic nature of arrivals and dwell times (Section 4.1) introduces temporal uncertainty in $a_{i,t}$.
To represent this at planning level, the expected availability $\bar{a}_{s,t}$ for each segment s is obtained as $\bar{a}_{s,t} = \mathbb{E}[\, a_{i,t} \mid s \,]$, and applied as a **probabilistic weighting** to the flexibility bounds.

Accordingly, the planning-level probabilistic flexibility bounds for node or charging-park j are defined as:

$$\tilde{P}_{j,t}^{\min} = \bar{a}_{s,t}\, P_{j,t}^{\min}, \quad \tilde{P}_{j,t}^{\max} = \bar{a}_{s,t}\, P_{j,t}^{\max}.$$

This scaling preserves the expected diversity of EV connections while producing a compact, planner-friendly representation of aggregate flexibility. It should be noted, however, that these envelopes represent expected-value ranges rather than guaranteed operational limits. For risk-based or reliability-oriented analyses, planners may instead derive quantile-based envelopes (e.g., 5th and 95th percentiles) from Monte Carlo simulations, ensuring that both typical and extreme scenarios are appropriately captured in probabilistic load-flow and hosting-capacity studies. The coupling with SoC is retained through **energy balance constraints**:

$$E_{i,t+1} = E_{i,t} + \eta_i^{ch} P_{i,t}^{+} \Delta t - \frac{P_{i,t}^{-} \Delta t}{\eta_i^{dis}},$$

With $E_{i,t}^{\min} \leq E_{i,t} \leq E_{i,t}^{\max}$ to ensure that flexibility activations remain physically feasible over multiple time steps.

4.5.2. Rebound and Deferred Energy Modelling

Activation-level flexibility often defers part of the charging energy, creating a **rebound or backlog effect** after the activation window. At planning scale, this is represented by a deferred-energy variable E_t^{def}:

$$E_{t+1}^{\mathrm{def}} = \left(E_t^{\mathrm{def}} + \Delta E_t^{\mathrm{act}}\right) \cdot (1 - r_{\mathrm{clr}}),$$

where:

- $\Delta E_t^{\mathrm{act}}$ is the energy curtailed during activation,
- r_{clr} is the backlog-clearing rate (typically 0.3–0.5 per hour).

This variable quantifies the **post-activation rebound** and allows planning models to respect both flexibility limits and energy-recovery constraints.

4.5.3. Aggregation and Correlation

When aggregating multiple EVSEs or depots, independent stochastic samples may over- or underestimate diversity. To preserve realistic aggregation effects, correlation matrices between arrival times, dwell durations, and response parameters $(\alpha_i, \beta_i, \gamma_i)$ are used to compute **diversity factors** D_s:

$$P_{j,t}^{\max,\mathrm{eff}} = D_s \sum_{i \in \mathcal{I}_j} P_{i,t}^{\max},$$

with typical D_s values between 0.6 (home) and 0.85 (workplace). These factors ensure that aggregated envelopes realistically reflect temporal overlap between individual EV availabilities.

4.6. Example Control

This subsection illustrates how the activation model from Sections 4.1 – 4.5 can be implemented and used to benchmark different flexibility services on a single EV charging park. The example is not calibrated to a specific pilot but demonstrates the workflow and the type of outputs exposed.

4.6.1. Simulation set-up

A 24-hour horizon is discretised at $\Delta t = 15$ minutes ($N = 96$ steps). We simulate $N_{\mathrm{EV}} = 300$ EV sessions connected to one charging park (with different characteristics), with the following segment shares: home 60 %, work 20 %, public 15 %, fleet 5 %.

For each EV i:

- arrival T_i^{arr} and departure T_i^{dep} are drawn from segment-specific distributions (Section 4.1);
- energy request E_i^{req} as indicated in Figure 2 and initial SoC $\mathrm{SoC}_{i,0}$ follow the conditional model in Section 4.2 for a cold day ($\theta = 5°\mathrm{C}$);

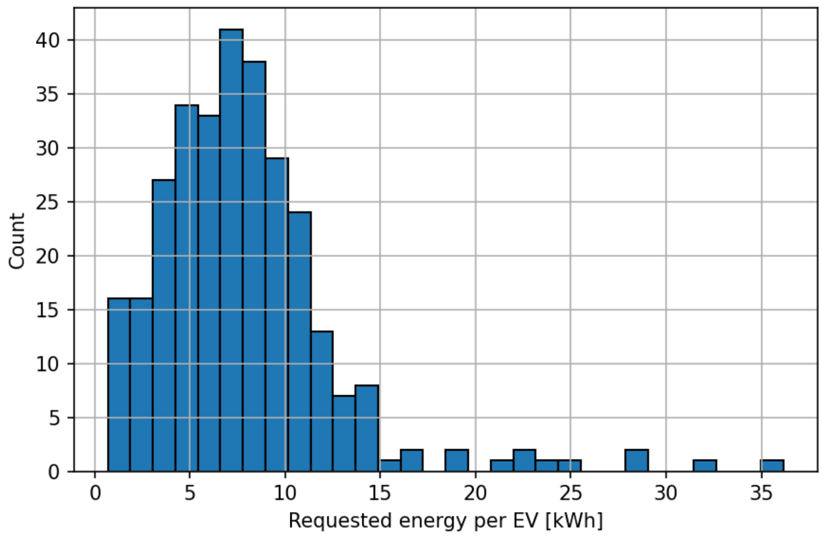

Figure 2: Histogram of simulated session-level energy requests E_i^{req} across all EVs, reflecting heterogeneity in trip lengths, battery sizes, and user segments used in the activation model.

- control mode is assigned as:
  - uncontrolled (baseline),
  - V1G smart charging,
  - a smaller share of V2G-capable users with export limit $P_i^{\mathrm{dis,max}}$ and minimum SoC $\mathrm{SoC}_i^{\min}$.

A **synthetic price profile** π_t (evening peak, low-price night) and a **simple congestion/control signal** c_t (penalising 18:00–21:00) are used as inputs for smart-charging modes.

We evaluate four flexibility services:

1. **None (uncontrolled)** — all EVs charge on arrival at P_i^{max} until E_i^{req} is met.
2. **Price-based V1G** — V1G users schedule charging in their availability window to minimise $\sum_t (\pi_t + c_t) P_{i,t}$.
3. **Price-based V2G** — a subset of EVs can discharge at high-price hours and recharge at low-price hours, respecting $\mathrm{SoC}_i^{\min}$ and final energy targets (example histogram is represented in Figure 3).
4. **Peak reduction service** — starting from smart/V2G schedules, an aggregator-level heuristic scales flexible loads to respect a peak cap and reallocates energy in uncongested periods.

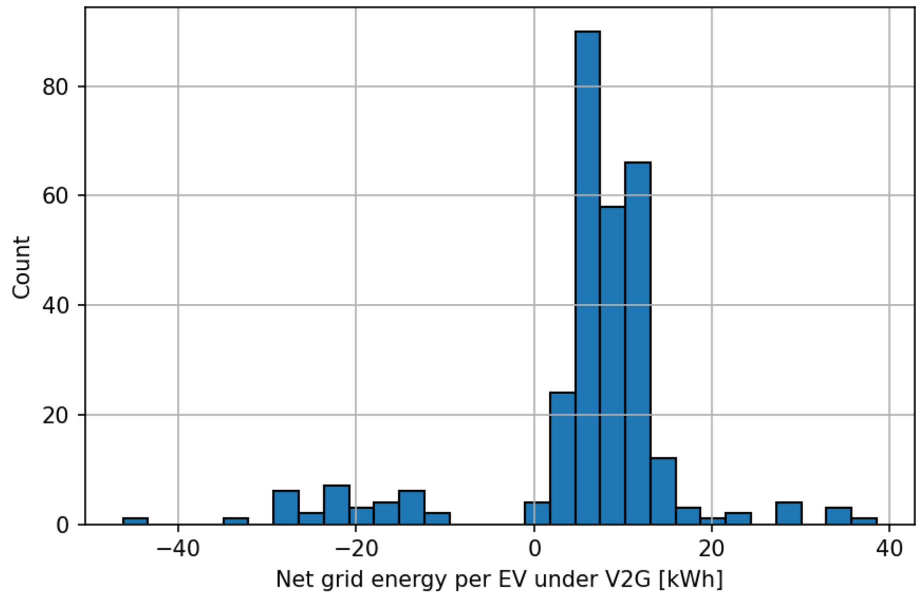

Figure 3: Histogram of net daily energy exchanged with the grid by V2G-capable EVs, highlighting the mix of net consumers and net providers resulting from the arbitrage and support actions within the V2G control strategy.

For each case, the aggregate profile $P_t^{agg} = \sum_i P_{i,t}$ is computed.

4.6.2. Activation Results

The resulting daily peak powers and total energies are (as shown on Figure 4):

- None (uncontrolled): $P_{\max} \approx 510$ kW, $E_{\text{day}} \approx 2.75$ MWh
- Price-based V1G: $P_{\max} \approx 498$ kW, $E_{\text{day}} \approx 2.61$ MWh

- Price-based V2G: $P_{\max} \approx 397$ kW, $E_{\text{day}} \approx 1.70$ MWh
- Peak reduction service: $P_{\max} \approx 356$ kW, $E_{\text{day}} \approx 1.58$ MWh

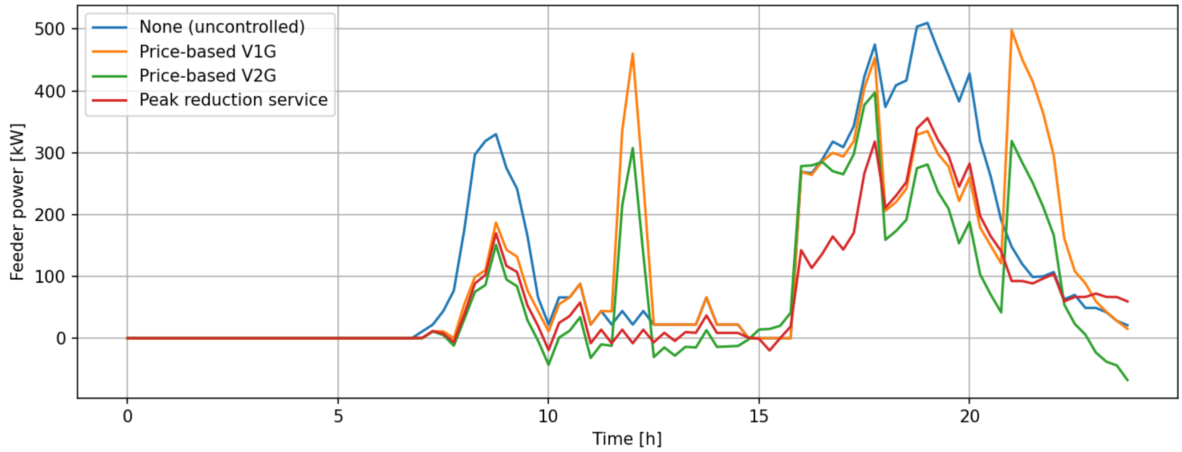

Figure 4: Daily power profile under four control modes: uncontrolled charging, price-based V1G, price-based V2G, and the coordinated peak-reduction service.

4.6.3. Planning results

The activation-level simulations can be aggregated into simplified representations that are suitable for planning studies. Instead of simulating each individual EV, the aggregate flexibility of the entire EV charging park can be expressed as upper and lower power envelopes $P_t^{\min}$ and $P_t^{\max}$. These represent, at each time step, the range of possible net power exchange resulting from the fleet of connected EVs.

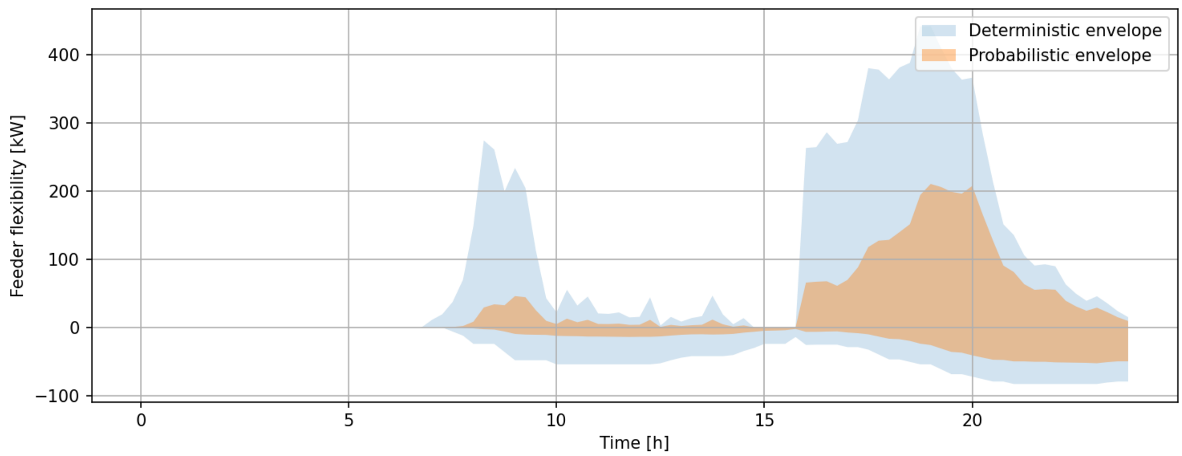

Figure 5: The figure presents the deterministic (worst-case) and probabilistic envalopes of the energy flexibility.

Two complementary envelope definitions are illustrated in Figure 5:

1. **Deterministic envelope (blue band)** — constructed from the activation model using energy- and SoC-feasible "earliest-charging" and "earliest-discharging" schedules. It

represents the physically attainable limits of charging-park-level power without allowing conflicting actions (i.e. no simultaneous early and late charging). This envelope captures the maximum charging and discharging potential that the EV fleet can provide at any instant, and it tightly bounds all simulated activation cases.

2. **Probabilistic envelope (orange band)** — obtained by scaling the deterministic envelope by the average availability of EVs at each time step, $\bar{a}_t$. It captures the *expected* flexibility that could realistically be activated, considering that not all EVs are simultaneously connected. The probabilistic envelope is therefore narrower and more representative of typical daily conditions.

5. CONCLUSIONS

This deliverable specifies the modelling framework and data structures that will serve as the foundation for the software developments in Task 3.4. Building on empirical evidence from EV charging sessions datasets, travel behaviour studies and recent EV–grid research, we formalised stochastic models for arrivals, dwell times, energy requests and initial state-of-charge across different contexts, explicitly accounting for seasonality and temperature effects. This core ensures that flexibility assessments are rooted in realistic usage patterns rather than stylised assumptions and providing a framework to build upon. This methodology is building a way that the individual elements (rebound effects, the temperature effects, the characteristics of the users, the individual clusters) can be added or not based on the availability of the data itself.

On top of this layer, we defined EV charging park flexibility representations that are directly compatible with congestion management, scheduling and planning tools. For activation timescales, we specified feasible trajectory sets under uncontrolled charging, unidirectional smart charging (V1G) and optional bidirectional (V2G) operation, exposing key quantities such as availability, ramping constraints and rebound risks. For planning applications, we translated these detailed activation models into reduced-order flexibility envelopes and probabilistic availability profiles remain computationally tractable over the horizon, while preserving SoC feasibility and multi-period coupling.

Deliverable D3.2 clarifies interfaces within the AHEAD architecture. It provides machine-readable probabilistic net-load profiles, flexibility envelopes and scenario sets suitable for probabilistic load-flow, reinforcement deferral and risk-based planning. The tool will be developed in the AHEAD project the Task 3.4 and will take this methodology as the basis for the development. Through these steps, the concepts introduced in this deliverable are transformed into operational, open, and reproducible methods that enable DSOs, aggregators and policymakers to plan and activate EV flexibility with confidence, while remaining compliant with GDPR and supporting the broader decarbonisation of European mobility and distribution grids.

6. BIBLIOGRAPHY

[1] C. Neuman, A. Meintz and M. Jun, “Workplace Charging Data Collection and Behavior,” National Renewable Energy Laboratory, Denver, 2021.

[2] E. Dudek, K. Platt, N. Storer, P. Barnfather and R. Duke, “Electric Nation Customer Trial Final Report,” Western Power Distribution Innovation, 2019.

[3] T. Garg, R. Hanna, J. Myers, S. Tebbe and D. G. Victor, “Electric Vehicle Charging at the Workplace: Experimental Evidence on Incentives and Environmental Nudges,” Munich Society for the Promotion of Economic Research - CESifo GmbH, Munich, Germany, 2024.

[4] M. Bailey, D. Brown, B. Shaffer and F. Wolak, “Show Me the Money! A Field Experiment on Electric Vehicle Charge Timing,” *American Economic Journal: Economic Policy,* vol. 17, no. 2, p. 259–84, 2025.

[5] EV.ENERGY MEDIA TEAM, “Dynamic Pricing Outperforms Time-of-Use in California EV Charging Pilot with 98% Energy Delivered Off-Peak,” EV Media, 2 June 2025. [Online]. Available: https://www.ev.energy/en-us/blog/dynamic-pricing-outperforms-time-of-use-in-california-ev-charging-pilot-with-98-energy-delivered-off-peak?utm_source=chatgpt.com.

[6] M. Muratori, “Impact of Uncoordinated Plug-in Electric Vehicle Charging on Residential Power Demand,” *Nature Energy,* vol. 3, no. 3, pp. 193--201, 2018.

[7] S. F. Daneshzand, P. Coker, B. Potter and S. T, “EV smart charging: How tariff selection influences grid stress and carbon reduction,” *Applied Energy,* vol. 348, no. 1, p. 121482, 2023.

[8] S. Birk Jones, W. Vining, M. Lave, T. Haines, C. Neuman, J. Bennett and D. R., “Impact of Electric Vehicle customer response to Time-of-Use rates on distribution power grids,” *Energy Reports,* vol. 8, pp. 8225-8235, 2022.

[9] T. Unterluggauer, H. F., S. Klyapovskiy and P. B. Andersen, “Impact of Electric Vehicle Charging Synchronization on the Urban Medium Voltage Power Distribution Network of Frederiksberg,” *World Electric Vehicle Journal,* vol. 13, no. 10, p. 182, 2022.

[10] Minnesota Department of Commerce, “Minnesota Department of Commerce Demand Response Impact Study,” Michael Energy, Minesota, 2013.

[11] H. Sæle, “Electric vehicles in Norway and the potential for demand response,” 11 Apr 2025. [Online]. Available: https://blog.sintef.com/energy/electric-vehicles-norway-demand-response/.

[12] B. Ross, K. Bocklund, M. Prorok, D. McFarlane, A. Finis, B. Jordan, J. Greene and K. Acuña, “Solar Power + Electric Vehicle Charging: Capturing Synergies in Minnesota,” NREL, Minesota, 2025.

[13] R. Horns, “NREL Research Finds the Right TEMPO for National Electric Vehicle Grid Planning,” NREL, 25 September 2023. [Online]. Available: https://www.nrel.gov/news/detail/program/2023/nrel-research-finds-the-right-tempo-for-national-electric-vehicle-grid-planning.

[14] L. Nursitihazlin, A. Termida, Y. O. Susilo, J. P. Franklin and C. , “Understanding seasonal variation in individual’s activity participation and trip generation by using four consecutive two-week travel diary,” *Travel Behaviour and Society,* vol. 12, pp. 52-63, 2018.

[15] P. Walsh, R. Isaac, R. Vijayagopal, A. Rousseau, J. Seo and N. Kim, “Impact of Cold Ambient Temperature and Extreme Conditions on Electric Vehicles,” Department of Energy - United States of America, 2024.

[16] E. Esparza, D. Truffer-Moudra and C. Hodge, “Electric Vehicle and Charging Infrastructure Assessment in Cold- Weather Climates: A Case Study of Fairbanks, Alaska,” National Renewable Energy Laboratory, 2025.

[17] M. Ali Reza Abbasi, “Probabilistic load flow in distribution networks: An updated and comprehensive review with a new classification proposal,” *Electric Power Systems Research,* vol. 222, p. 109497, 2023.

[18] R. M. Salehi and M. Mahdi, “An improved probabilistic load flow in distribution networks based on clustering and Point estimate methods,” *Energy and AI,* vol. 14, p. 100272, 2023.

[19] J. Dupačová, N. Gröwe-Kuska and W. Roemisch, “Scenario reduction in stochastic programming An approach using probability metrics,” *Mathematical Programming,* vol. 95, pp. 493-511, 2003.

[20] H. Heitsch and W. Roemisch, “Scenario tree reduction for multistage stochastic programs,” *Computational Management Science,* vol. 6, pp. 117-133, 2009.

[21] K. Poncelet, H. Höschle, E. Delarue, A. Virag and W. D’haeseleer, “Selecting Representative Days for Capturing the Implications of Integrating Intermittent Renewables in Generation Expansion Planning Problems,” *IEEE Transactions on Power Systems,* vol. 32, no. 3, pp. 1936-1948, 2017.

[22] H. Teichgraeber and A. R., “Clustering methods to find representative periods for the optimization of energy systems: An initial framework and comparison,” *Applied Energy,* vol. 239, pp. 1283-1293, 2019.

[23] E. S. Lázaro and L. M. Serra, “Evaluation of methods to select representative days for the optimization of polygeneration systems,” *Renewable Energy,* vol. 151, pp. 488-502, 2020.

[24] C. D. W. Wanninayaka , K. N. Hasan, A. Vahidnia and M. T. Rahman, “Probabilistic coupled EV-PV hosting capacity analysis in LV networks with spatio-temporal modelling and copula theory,” *IET Smart Grid,* vol. 7, no. 6, pp. 917-928, 2024.

[25] C. Bian, H. Li, F. Wallin, A. Avelin, L. Lin and Z. Yu, “Finding the optimal location for public charging stations – a GIS-based MILP approach,” *Energy Procedia,* vol. 158, pp. 6582-6588, 2019.

[26] S. Çelik and Ş. Ok, “Electric vehicle charging stations: Model, algorithm, simulation, location, and capacity planning,” *Elsevier,* vol. 10, no. 7, pp. 2405-8440, 2024.